Current Microbiology
https://doi.org/10.1007/s00284-020-02040-0

# Rapid Detection of *Escherichia coli* by β-Galactosidase Biosensor Based on ZnO NPs and MWCNTs: A Comparative Study

**Rafieh Meraat[1] · Khosro Issazadeh[1] · Ali Abdolahzadeh Ziabari[2] · Mohammad Faezi Ghasemi[1]**

Received: 3 January 2020 / Accepted: 18 May 2020


**Abstract**
The need for alternative approaches for identifying pathogens has led researchers to focus on nanobiotechnology. In this study, zinc oxide nanoparticles (ZnO NPs) and multi-wall carbon nanotubes (MWCNTs) were used as marker molecules. After measuring the best concentration of these nanomaterials to inhibit the lactase activity of the beta-galactosidase enzymes by binding to them, different concentrations of *Escherichia coli* were added to the medium and their detection ability was finally compared with each other. Due to small size and high reactivity, these compounds are able to detect very low amount of bacteria in the ambient. In fact, the bacteria are attached to the nanoparticles and detach them from the enzyme and lead to substrate decomposition by the enzyme. MWCNTs exhibited better performance than ZnO NPs in detection of bacteria at very low concentration of $10^1$ CFU/ml in 15 min. As a result, they are very appropriate to be utilized especially in the food industry.

## Introduction

Over the past few decades, microbial pathogens have been the main reason of many infections, diseases, and even deaths across the world. Therefore, it is very important to recognize and identify these microbial agents particularly in agricultural and food industries [1, 2] where the main goal is to produce healthy foods and drinks [3]. Traditional culture methods to detect microbial contaminations are very time-consuming and the related equipment is so delicate [4]. On the other hand, some infections require rapid diagnosis, detection, and treatment that can be clinically important and critical. Indeed, the time it takes to diagnose a disease is very effective in saving a person's life, and if an illness is detected late, it may lead to serious complications [5]. *Escherichia coli* (*E. coli*) is an indicator of microbial contaminations that is usually found in foods. Therefore, the diagnosis of this bacterium in food industries is considered as one of the health criteria [6]. As was mentioned above, some microbiological tests like multiple tube fermentation (MTF), membrane filter (MF), Plate Count Methods, PCR and ELISA are available to identify and count bacterial levels in water and other resources. However, using these methods takes several days especially in cases which the bacteria concentration in the sample is trace [7, 8]. Hence, alternative methods for detection of microbial contaminations of food, sewage, human and animal populations are needed. Recent advances in nanotechnology have led to the development and emergence of new diagnostic systems with high specificity and sensitivity to detect pathogens. For instance, based on advanced organic reactions, enzymatic nano biosensors can detect microbial contamination in food in a short time [1]. Biosensors are analytical tools. The main parts of a common biosensor are: (1) a bioreceptor for doing interaction with the target analyte, and (2) a transducer to convert the performed interaction into an electronic signal [2]. The first biosensor was invented by Clark and Lyons in 1962 [9].

The incompatibility between analyte molecule and transducer material is often a critical issue in biosensors. Covalent immobilization, physical adsorption and cross-linking with other components, have been proposed to exceed this problem [10, 11]. Based on conversion mechanism, biosensors are divided into several categories such as electrochemical, optical, piezoelectric and thermo-calorimetric. Amongst all types of biosensors, the electrochemical biosensors are very popular [12]. A biosensor can sense a specific type of a biological substance

✉ Ali Abdolahzadeh Ziabari
ali.abd.ziabari@gmail.com; ali_abdolahzadeh@liau.ac.ir

[1] Department of Microbiology, Faculty of Sciences, Lahijan Branch, Islamic Azad University, Lahijan, Iran

[2] Nano Research Lab, Lahijan Branch, Islamic Azad University, PO. Box: 1616, Lahijan, Iran

Published online: 22 May 2020

that normally contains antibodies, proteins, enzymes, immunological molecules, etc. [13]. Commonly, in an electrochemical biosensor, the immobilized enzymes are used because of having high specificity for analyte molecules and making an appropriate connection between the target molecule and the transducer [10]. The hydrolytic beta-galactosidase (β-gal) enzyme is a kind of diagnostic enzyme that produces glucose and galactose from lactose hydrolase [14]. Owing to their high chemical, mechanical and thermal stability, nanostructured metal oxide semiconductors have recently attracted great interests in point of care (POC) diagnostics [15]. Besides, nanostructured semiconducting materials facilitate electron transport that is a crucial issue in biosensors. Among all semiconducting metal oxides, the safe and earth-abundant ZnO material has unique features at room temperature including wide bandgap of 3.37 eV, large bond strength, large exciting binding energy (60 meV) and piezoelectric properties. So far, lots of studies have been devoted to investigate nanostructured ZnO-based biosensors for detection of glucose, uric acid, DNA and cancer biomarkers [16]. Carbon nanotubes (CNTs) have unique features including high surface area, high thermal and mechanical resistance, great electrical characteristics, excellent biocompatibility and high sensitivity that make them very attractive for applications in many fields [17]. MWCNTs and ZnO nanostructures have shown very promising sensing properties [18]. In the present study, nanostructures of cationic ZnO and carbon nanotube were used to inhibit β-gal activity. The main goal of this study is to describe the development of a selective and sensitive method for monitoring *E. coli* by using of ZnO nanoparticles (NPs) and MWCNTs. Meanwhile, a comparison will be made between the strength and sensitivity of the prepared ZnO NPs and the functionalized MWCNTs to detect the bacteria.

## Experimental

### Materials and Chemicals

The chemicals used for synthesis of ZnO NPs were zinc acetate dehydrate (cat. no. 1.08802(, methanol (cat. no. 1.06007) and diethanolamine (DEA, cat. no. 8.03116) purchased from Merck. Beta-galactosidase (cat. no. N1127), glutaraldehyde (cat. no. 354400) and *ortho*-nitrophenyl-β-galactoside (cat. no. 48277) were purchased from Sigma-Aldrich. EMB agar (cat. no. 1.01347), LB broth (cat. no. 1.10285) and LB agar (cat. no. 1.10283) medium were used as the growth medium for bacteria and were purchased from Merck.

### Synthesis of ZnO NPs

Sol–gel wet chemical method was used to fabricate ZnO NPs. Initially, 2.5 g of zinc acetate was weighed and mixed well in 30 ml of methanol by using a magnetic stirrer for 0.5 h. Then, 1 ml of DEA was blended well in zinc acetate solution under continuous stirring for 1 h. Hydrolysis process occurred when the resultant transparent sol was left for 24 h at room temperature. Subsequently, the produced yellow gel was annealed in air at a furnace at temperature of 550 °C for 2 h. Eventually, ZnO NPs were obtained.

### Surface Modification of MWCNTs via Glutaraldehyde

In this study, glutaraldehyde was used as a linker for β-galactosidase to improve the reactivity of MWCNTs. Glutaraldehyde is an appropriate linker for cross-linking of β-gal molecules. Glutaraldehyde-bonded carbon nanotubes are also capable of binding anionic compounds. Amine group of the enzyme, also participates in this junction. In the present study, 5 g of MWCNTs were washed initially with deionized water and then centrifuged for 15 min at 2000 rpm. Then, supernatant (liquid at the top of the tube after centrifugation) was removed. Afterward, 5 ml of glutaraldehyde (0.5 M) in buffer was added quickly to the pellet. The tubes then were covered and shacked for 7 h at a speed of 150 rpm. After that, glutaraldehyde traces were removed by centrifugation (15 min, 2000 rpm). After decanting of supernatant, the pellet was washed twice with deionized water and Assay buffer (100 mM PBS, pH 7.0).

### Characterization

Structural study of the samples was carried out by X-ray diffraction (XRD) technique using a XRD 6000, Shimadzu apparatus with $CuK_{\alpha}$ radiation ($\lambda = 0.15406$ nm). Fourier transform infrared spectroscopy (FTIR) absorption was measured for KBr-supported samples over the frequency range of 400–4000 $cm^{-1}$ and at a resolution of 5 $cm^{-1}$, using a model Spectrum Two from PerkinElmer Company. The diameter and size distribution of NPs were measured by a transmission electron microscope (TEM) (Zeiss-EM10C-100 kV, Germany). The pertinent concentrations were measured by using UV–Vis diffuse reflectance spectroscopy DRS (UV-2550 SHIMADZU, Japan).

### Enzyme Activity Evaluation

Enzyme activity measurement was performed based on the referenced method of Sigma-Aldrich Company. The activity of a unit (1U) of the β-gal enzyme is called a portion

of the enzyme that decomposes one micromole of *ortho*-nitrophenyl-β-galactoside at 25 °C (ONPG) per min and pH 7, according to the following reaction:

$$\text{ONPG} + \beta\text{-D-Galactopyranoside} + H_2O \rightarrow \text{o-Nitrophenol} + \beta\text{-D-Galactose}.$$

### β-Gal Activity Assay in the Presence of a Nanoparticle

β-Gal enzyme activity was measured both for ZnO NPs and MWCNTs, separately. Assay was performed in a 96-well plate. Various concentrations of nanoparticles (10–130 µl) were mixed with 40 µl of β-gal in different wells. Using PBS, 200 µl of each mixture was prepared. The plate then was incubated at 37 °C for 30 min. After this time, a constant amount of ONPG (10 µl) was added to each home. Then, the absorbance of each well was recorded at 405 nm every 20 s for 30 min. That concentration of nanoparticle that caused stopping the enzyme activity was selected to be used in bacterial identification and diagnostic step.

### Culture and Preparation of Different Concentrations of Bacteria

Standard bacterial cultures *Escherichia coli* PTCC 1533 were procured from the Persian Type Culture Collection. The bacterial culture was streaked to check the purity, and a single colony was inoculated in the selective medium of EMB agar (Eosin methylene blue). A colony of cultured *E. coli* was inoculated from the agar plates to sterilize LB broth (Luria Broth) medium in the tubes and incubated at 37 °C for 24 h. Then, the obtained bacteria were diluted with tenfold serial dilutions. Nearly 100 µl of each tube was inoculated on the surface of LB agar and cultured in 37 °C for 24 h. Afterward, colonies were counted in each plate followed by using appropriate dilution factors to achieve $10^1$–$10^8$ CFU/ml.

### Bacteria Detection

During microorganism's detection in liquid samples by electrical reactions, the presence of various ions may cause false-positive reactions. Therefore, the PBS buffer was used as the reaction medium. To perform the detection process, 40 µl of β-galactosidase enzyme was mixed separately with ZnO NPs and MWCNTs in 96-well plate. Then, different concentrations of bacteria ($10^1$–$10^8$ CFU/ml) were inoculated in each well. To give enough time to the bacteria and the enzyme for binding to ZnO NPs and MWCNTs, the plates were incubated at 37 °C for 30 min. Then, the constant amount of ONPG added to each well (30 µl). Finally, the absorption spectra were recorded at the wavelength of 405 nm after 15 and 30 min.

## Results and Discussion

### Structural & Optical Study of the Synthesized ZnO NPs and MWCNTs

Figure 1 illustrates the XRD patterns of the prepared ZnO NPs and the functionalized MWCNTs. It is evident that three diffraction peaks of (100), (002) and (101) corresponding

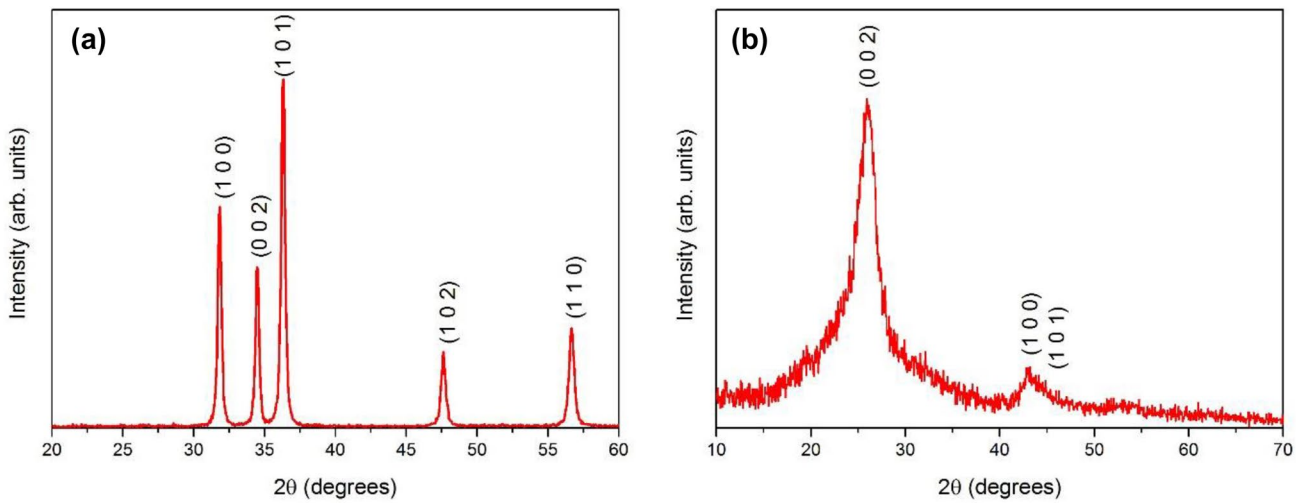


**Fig. 1** X-ray diffraction patterns for **a** ZnO NPs and **b** MWCNTs

to the wurtzite structure are dominant for ZnO NPs. The observed sharp diffraction peaks imply the good crystallinity of the sample. The evaluated grain size of the NPs by the well-known Scherer's formula [19] was 23 nm (Fig. 1a). This is in very good agreement with TEM result (Fig. 2a).

Diffraction pattern of MWCNTs displays an intense diffraction peak around $2\theta = 26^{\circ}$ corresponding to (002) orientation (Fig. 1b). Low intense diffraction peaks around 43°, and 44° can be assigned to (100) and (101) diffraction planes of MWCNTs, respectively [20, 21].

As it comes from the TEM micrograph of MWCNTs, the nanotubes of carbon have been distributed evenly with the radius lower than 10 nm (Fig. 2b).

The FTIR spectrum of ZnO nanoparticles in the range of 400–4000 $cm^{-1}$ has been depicted in Fig. 3a. The strong peak in 3430 $cm^{-1}$ is related to O–H stretching and bending vibrations of adsorbed water molecules on ZnO [18]. The peaks around 1632 $cm^{-1}$ and 1381 $cm^{-1}$ are corresponding to asymmetric and symmetric C=O bonds vibrations, respectively [22]. Figure 3b shows the FTIR spectra for pure and functionalized MWCNTs. The observed peak at 1390 $cm^{-1}$ for pure and carboxyl functionalized MWCNTs is assigned to C–N stretching mode [23]. The strong peak at 1630 $cm^{-1}$ corresponds to the stretching mode of C=C double bond that forms the framework of the carbon nanotube sidewall [24]. Results show that the corresponding FTIR peaks for the carboxyl functionalized sample are stronger than the pristine (non-functionalized) MWCNTs indicating the effective incorporation of carboxyl group.

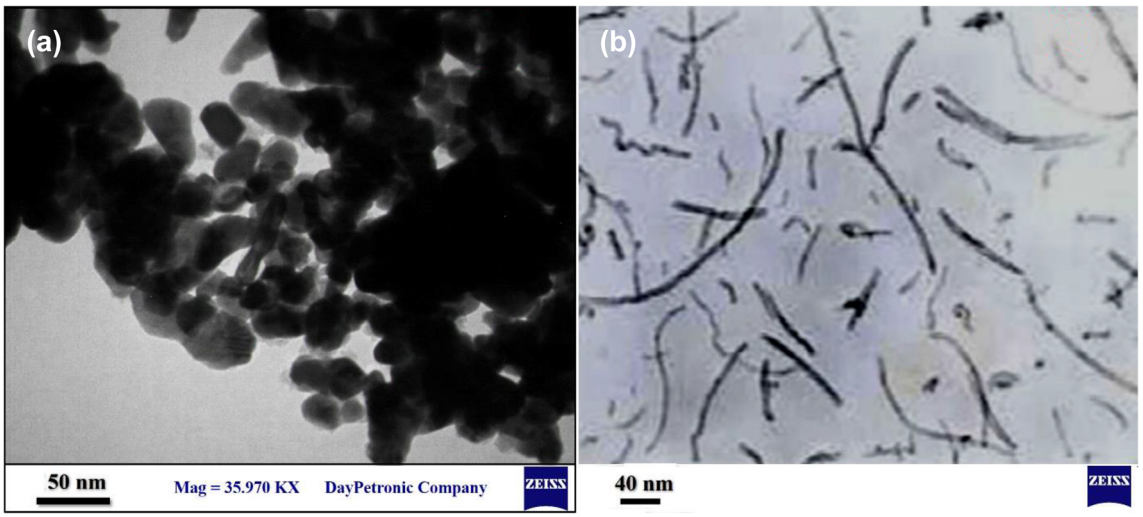


**Fig. 2** Representative TEM images of **a** ZnO NPs and **b** MWCNTs

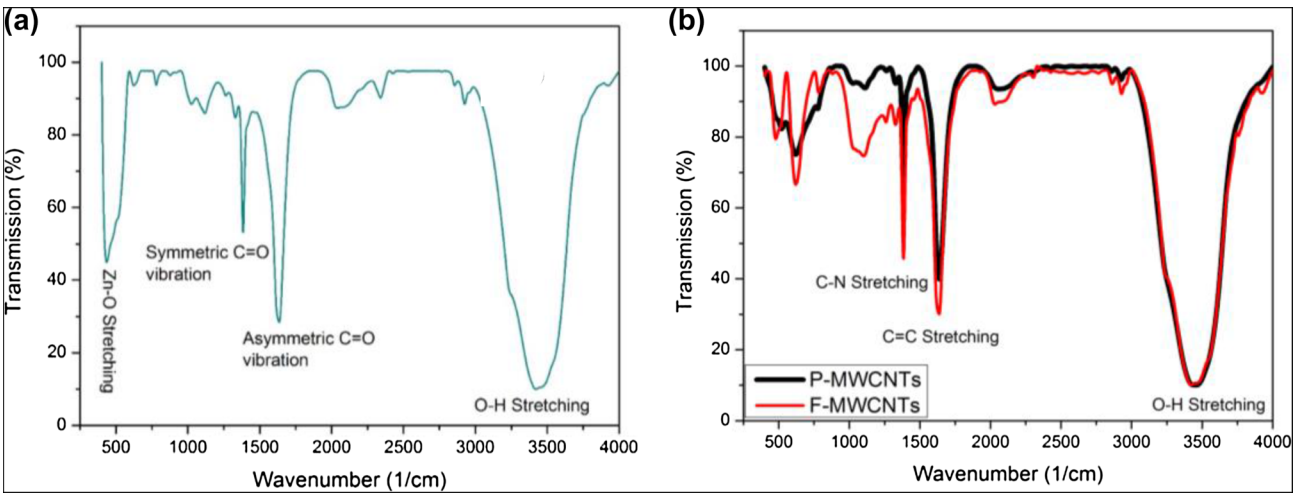


**Fig. 3** FTIR spectra for ZnO NPs (**a**), pure MWCNTs and carboxyl functionalized MWCNTs (**b**)

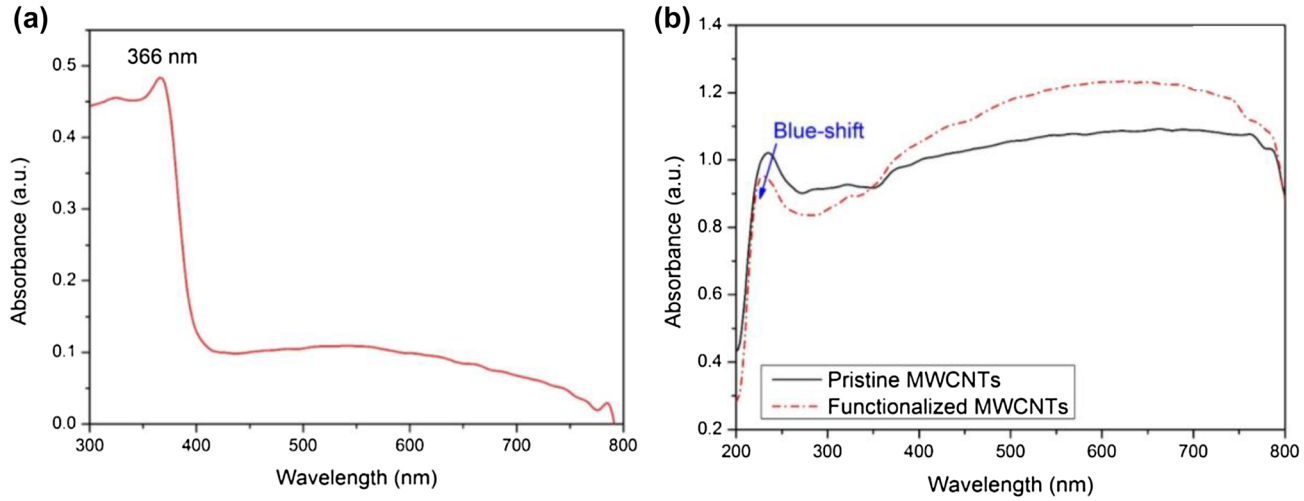


**Fig. 4** The room temperature UV–Vis DRS of ZnO nanoparticles (**a**), pristine and carboxyl functionalized MWCNTs (**b**)

Figure 4a indicates the UV–Vis DRS spectrum of ZnO NPs. It is seen that the absorption edge occurs at 366 nm corresponding to 3.39 eV. This exhibits a blue-shift relative to the bulk value for ZnO (3.30 eV) indicating the formation of nanostructures that cause the quantum confinement effect. The UV–Vis DRS spectra for pristine and functionalized MWCNTs have been displayed in Fig. 4b. Both spectra contain a major absorption peak at 234 nm corresponding to the reported absorption edge for MWCNTs [25]. After incorporating the carboxyl to the pristine MWCNTs the absorption peak underwent a blue-shift and was found around 229 nm. This indicates that, the functionalized form of MWCNTs can cover wider range of UV–Vis region.

## β-Galactosidase Activity Assay in the Presence of a ZnO NPs and MWCNTs

The optimum pH for *Kluyveromyces fragilis* β-galactosidase function is 6.5, 6.6 and 7 in optimum temperature of 30–35 °C [26]. So, all experiments were performed in neutral pH. The amount of enzyme that was able to completely dissolve the ONPG substrate was 60 µl. This amount was used for the β-galactosidase activity assay in the presence of ZnO NPs and MWCNTs.

To keep nanoparticles well-dispersed and stable in solutions, different dispersants were opted to modify the surface of NPs [27]. The facile traditional stirring was used for reduction of electrostatic steric hindrance between NPs.

The results show that MWCNTs are more effective than ZnO NPs in inhibition of β-gal activity. MWCNTs inhibited β-gal activity in the volume of 80 µg/well, whereas ZnO NPs inhibited enzyme function in 50 µg/well. These values were used for detection of bacteria. Because of the hydrophobic properties of MWCNTs, the reactivity between the MWCNTs and the enzyme is mediated by hydrophobic amino acids in enzymatic accumulation. However, due to partitioning effect, the reactivity will increase in a hydrophilic environment like an aqueous buffer. In addition to hydrophobic interaction, the π electrons of MWCNTs surface interact with the corresponding electrons of aromatic ring of amino acids such as phenylalanine and tryptophan and thus give rise enzyme adsorption on MWCNTs [28]. By increasing the amount of ZnO NPs and MWCNTs, the activity of the enzyme was stopped (Tables 1 and 2). This

**Table 1** Absorbance (a.u.) of β-galactosidase/ONPG in the presence of different concentrations of ZnO NPs

| Time (min) | ZnO NPs (µg/well) | | | | | | | | | | | | | |
|---|---|---|---|---|---|---|---|---|---|---|---|---|---|---|
| | 0 | 10 | 20 | 30 | 40 | 50 | 60 | 70 | 80 | 90 | 100 | 110 | 120 | 130 |
| 0 | 0/47 | 0/45 | 0/45 | 0/45 | 0/44 | 0/43 | 0/43 | 0/43 | 0/4 | 0/35 | 0/32 | 0/31 | 0/31 | 0/3 |
| 5 | 0/56 | 0/53 | 0/51 | 0/49 | 0/48 | 0/45 | 0/44 | 0/42 | 0/41 | 0/36 | 0/34 | 0/33 | 0/33 | 0/33 |
| 10 | 0/73 | 0/67 | 0/61 | 0/58 | 0/55 | 0/52 | 0/51 | 0/48 | 0/43 | 0/37 | 0/36 | 0/35 | 0/34 | 0/34 |
| 15 | 0/85 | 0/79 | 0/72 | 0/69 | 0/66 | 0/63 | 0/61 | 0/59 | 0/53 | 0/37 | 0/36 | 0/35 | 0/34 | 0/34 |
| 20 | 0/92 | 0/86 | 0/81 | 0/76 | 0/69 | 0/65 | 0/6 | 0/56 | 0/54 | 0/38 | 0/37 | 0/36 | 0/35 | 0/34 |
| 25 | 1/09 | 0/98 | 0/9 | 0/81 | 0/77 | 0/7 | 0/65 | 0/58 | 0/55 | 0/38 | 0/37 | 0/36 | 0/35 | 0/35 |
| 30 | 1/28 | 1/12 | 1/03 | 1/01 | 0/95 | 0/91 | 0/89 | 0/88 | 0/86 | 0/38 | 0/37 | 0/37 | 0/36 | 0/35 |

**Table 2** Absorbance (a.u.) of β-galactosidase/ONPG in the presence of different concentrations of MWCNTs

| Time (min) | MWCNTs (μg/well) | | | | | | | | | | | | | |
|---|---|---|---|---|---|---|---|---|---|---|---|---|---|---|
| | 0 | 10 | 20 | 30 | 40 | 50 | 60 | 70 | 80 | 90 | 100 | 110 | 120 | 130 |
| 0 | 0/47 | 0/41 | 0/41 | 0/41 | 0/39 | 0/38 | 0/32 | 0/31 | 0/31 | 0/31 | 0/31 | 0/3 | 0/3 | 0/3 |
| 5 | 0/56 | 0/45 | 0/46 | 0/43 | 0/41 | 0/4 | 0/32 | 0/33 | 0/32 | 0/32 | 0/32 | 0/31 | 0/3 | 0/3 |
| 10 | 0/73 | 0/49 | 0/49 | 0/49 | 0/43 | 0/41 | 0/33 | 0/33 | 0/32 | 0/32 | 0/31 | 0/31 | 0/31 | 0/3 |
| 15 | 0/85 | 0/55 | 0/55 | 0/53 | 0/5 | 0/43 | 0/35 | 0/34 | 0/33 | 0/33 | 0/31 | 0/31 | 0/31 | 0/31 |
| 20 | 0/92 | 0/65 | 0/62 | 0/61 | 0/58 | 0/52 | 0/38 | 0/36 | 0/34 | 0/34 | 0/31 | 0/31 | 0/31 | 0/31 |
| 25 | 1/09 | 0/74 | 0/71 | 0/69 | 0/65 | 0/6 | 0/4 | 0/39 | 0/37 | 0/35 | 0/32 | 0/31 | 0/31 | 0/3 |
| 30 | 1/28 | 0/87 | 0/86 | 0/84 | 0/76 | 0/71 | 0/42 | 0/41 | 0/39 | 0/36 | 0/32 | 0/31 | 0/3 | 0/34 |

happens when the positive-charge NPs attach to the negative charge β-galactosidase enzyme and detach it from the substrate and inhibit its catalytic activity. This will stop the parsing of the ONPG into ONP (*o*-nitrophenol) and decrease the absorbance of the aqueous medium. Over the time, these activities intensify (Fig. 5a).

## Bacteria Detection

Detection and diagnosis of *E. coli* is a crucial factor in keeping the health of the community. *E. coli* is a type of gram-negative bacterium that is identified to be the most significant pathogenic agent in the family of *Enterobacteriaceae*

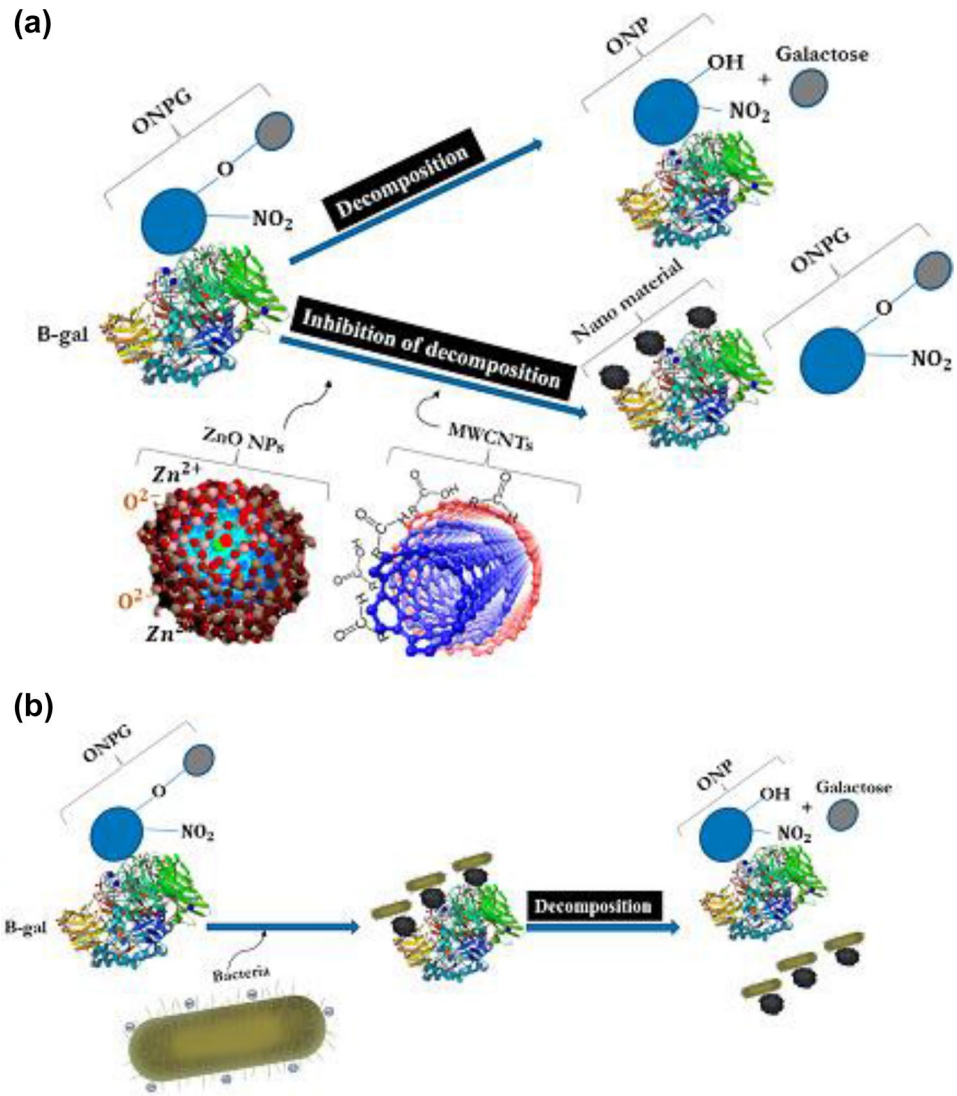


**Fig. 5** Schematic illustration of **a** enzymatic function of β-galactosidase in the presence and absence of NPs and **b** bacteria detection. β-gal enzymes break down ONPG to ONP. Binding of NPs to the enzyme, inhibits the enzyme activity and the substrate is removed from the enzyme. In the presence of bacteria, the NPs are bonded to the bacteria and the enzyme starts to break down the substrate

[29]. Hence, rapid detection of *E. coli* is an inevitable necessity for public health. Lots of studies suggest that the bacteria have a negative charge level. This can be proven by electrostatic interaction chromatography (ESIC). Gram-positive bacteria have a cell wall composed of a thick layer of peptidoglycan, which teichoic acid is one of its components. In gram-negative bacteria, peptidoglycan has a lipopolysaccharide (LPS). Indeed, the negative charge of bacteria comes from these compounds and positive-charge nanoparticles can be linked to bacteria by electrostatic reactions [30]. Li et al., Compared the *E. coli* binding capacity of positively charged $Fe_3O_4$ NPs (NP+) to negatively charged fluorescent NPs (NP−). After incubation bacterial suspension with different amounts of NP+ or NP− and magnetic separation by the nanoparticles, total solution was then analyzed for bacterial concentration via a plate counting method. They found that the positive charge of NP + can influence the bacterial capture efficiencies and NP− did not show affinities towards *E. coli.* They managed to capture *E. coli* at concentrations of 10 and 100 CFU/ml using NP+ within 1 h [30]. In our study, we have presented a faster way to capture of *E. coli* based on the strong electrostatic interaction between the surface of bacteria and the synthesized ZnO NPs and functionalized MWCNTs. After incubation of NPs/β-gal/bacteria complex, the bacteria are attached to the surface of the nanoparticles. The electrostatic interaction between the bacteria and NPs is stronger than the interaction between the enzyme and NPs. So, the enzyme will be released and attached to the substrate and starts to decompose it. As a result, the turbidity of the environment increases that indicates the beginning of the enzyme activity (Fig. 5b). Therefore, the detection point of the bacteria is the point that the adsorption value increases abruptly. Hence, it can be easily found that the faster detection will occur for the higher bacterial concentration and longer time. As the time gets longer, a greater number of microorganisms and so the greater number of ONP molecules in the medium are identified and result in adsorption enhancement. In this study, MWCNTs showed much better results than ZnO NPs in identifying the bacteria. When the bacteria concentration was 10 CFU/well, no change was observed in the ambient turbidity in the presence of ZnO NPs. However, the turbidity increased as the concentration of the bacteria increased (Table 3). This change was observed for MWCNTs at the concentration of 10 CFU/well. The adsorption values at 10 CFU of bacteria for MWCNTs are higher than the adsorption values in the absence of the bacteria. In fact, at the same concentration and at the same period of the time (15 min), MWCNTs could detect bacteria at very low concentration of 10 CFU/ml (Table 4), while this value was 100 CFU/ml for ZnO NPs. Besides, the substrate was not degraded by enzyme in the presence of bacteria. Over the time, it can be seen that the inhibitory effect of nanomaterials on enzyme activity reduces while the absorbance increases.

The accuracy and speed of bacterial recognition depend on the surface area, concentration, and reactivity of nanomaterials.

High surface-to-volume ratio, nontoxicity, good compatibility, chemical stability and proper electron exchange, make ZnO NPs very suitable for use in biosensors. On the other hand, carbon nanotubes have an ultrahigh surface area, mechanical strength, and excellent electrical conductivity that make them very efficient in reactivity and application in various fields [31]. A wide range of superficial surface area in carbon nanotubes provides the ability to immobilize a large number of compounds at their surface. MWCNTs have a diameter between 2 and 100 nm and are suitable for detecting target molecules via electrochemical reactions and connect and accumulate analytes [32]. Results of the present study show that the detection ability of MWCNTs is much better than that of ZnO NPs. This can be assigned to the higher surface-to-volume ratio of MWCNTs that improves the electron movement and reactivity. Above all, they have the ability of being connected more efficiently and broadly

**Table 3** Absorbance (a.u.) of β-galactosidase/ZnO NPs complex in the presence of different concentrations of bacteria

| Time (min) | Bacteria (CFU/well) | | | | | | | | |
|---|---|---|---|---|---|---|---|---|---|
| | 0 | 10 | $10^2$ | $10^3$ | $10^4$ | $10^5$ | $10^6$ | $10^7$ | $10^8$ |
| 0 | 0/36 | 0/36 | 0/41 | 0/42 | 0/42 | 0/43 | 0/43 | 0/43 | 0/44 |
| 15 | 0/43 | 0/43 | 0/53 | 0/59 | 0/64 | 0/67 | 0/72 | 0/75 | 0/8 |
| 30 | 0/73 | 0/73 | 0/76 | 0/81 | 0/87 | 0/89 | 0/96 | 1/08 | 1/19 |

**Table 4** Absorbance (a.u.) of β-galactosidase/MWCNTs complex in the presence of different concentrations of bacteria

| Time (min) | Bacteria (CFU/well) | | | | | | | | |
|---|---|---|---|---|---|---|---|---|---|
| | 0 | 10 | $10^2$ | $10^3$ | $10^4$ | $10^5$ | $10^6$ | $10^7$ | $10^8$ |
| 0 | 0/36 | 0/44 | 0/45 | 0/45 | 0/45 | 0/46 | 0/47 | 0/47 | 0/47 |
| 15 | 0/43 | 0/52 | 0/62 | 0/66 | 0/75 | 0/8 | 0/82 | 0/83 | 0/83 |
| 30 | 0/73 | 0/81 | 0/89 | 0/94 | 0/99 | 1/16 | 1/21 | 1/22 | 1/22 |

to the bacteria and enzyme. This is a crucial factor that increases the speed of bacterial detection. Altogether, considering the time and bacteria concentration, the prepared nanostructures showed rapid detection of *E. coli*.

## Conclusion

In summary, the sol–gel derived ZnO NPs and the functionalized MWCNTs were used for rapid detection of trace concentrations of *E. coli*. The structural analysis of the nanostructures was performed by XRD. TEM micrographs were taken to study the surface structure of the prepared samples. FTIR spectra were used to identify the functional groups that existed in the samples. The room temperature UV–Vis DRS spectra were recorded to study the wavelength dependence of the absorbance of the samples. The prepared nanostructures were used to detect *E. coli* based on β-gal/nanomaterials complex. From bacteria detection analysis, both ZnO NPs and functionalized MWCNTs showed high detection ability for low concentrations of *E. coli* and the lowest detected bacteria concentration of 10 CFU/ml was observed for MWCNTs. The detection procedure was performed rapidly and simply with high-precision needless to complicate instruments. The results of the present study can be useful for detection of both gram-negative and gram-positive bacteria in food industries, hospitals, and environmental topics rather than the time-consuming traditional methods.

## References


1. Jannat Y, Mohammed Raju A, Byoung-Kwan C (2016) Biosensors and their applications in food safety: a review. J Biosyst Eng 41:240–254. https://doi.org/10.5307/JBE.2016.41.3.240
2. Mehrotra P (2016) Biosensors and their applications: a review. J Oral Biol Craniofac Res 6:153–159. https://doi.org/10.1016/j.jobcr.2015.12.002
3. Ahari H (2014) The *Staphylococcus aureus* exotoxin recognition using a Sensor designed by nanosilica and SEA genotyping by multiplex PCR. Appl Food Biotechnol 1:37–44. https://doi.org/10.22037/afb.v1i1.7126
4. Chai Y, Horikawa S, Simonian A, Dyer D, Chin BA (2013) Wireless magnetoelastic biosensors for the detection of *Salmonella* on fresh produce. Proc Int Conf Sens Technol ICST 204:174–177
5. Ahmed A, Rushworth JV, Hirst NA, Millner PA (2014) Biosensors for whole-cell bacterial detection. Clin Microbiol Rev 27(3):631–646. https://doi.org/10.1128/CMR.00120-13
6. Choi Y et al (2018) Rapid detection of *Escherichia coli* in fresh foods using a combination of enrichment and PCR analysis. Korean J Food Sci Anim Resour 38:829–834. https://doi.org/10.5851/kosfa.2018.e19
7. Yamada K, Kim CT, Kim JH, Chung JH, Lee HG, Jun S (2014) Single walled carbon nanotube-based junction biosensor for detection of *Escherichia coli*. PLoS ONE. https://doi.org/10.1371/journal.pone.0105767
8. Ali MA, Eldin TAS, Moghazy GME, Tork IM, Omara II (2014) Original research article detection of *E. coli* O157: H7 in feed samples using gold nanoparticles sensor. Int J Curr Microbiol Appl Sci 3(6):697–708
9. Clark LC, Lyons C (1962) Electrode systems for continuous monitoring in cardiovascular surgery. Ann N Y Acad Sci 102:29–45. https://doi.org/10.1111/j.1749-6632.1962.tb13623.x
10. Nguyen HH, Lee SH, Lee UJ, Fermin CD, Kim M (2019) Immobilized enzymes in biosensor applications. Materials. https://doi.org/10.3390/ma12010121
11. Lerner MB, Goldsmith BR, McMillon R, Dailey J, Pillai S, Singh SR, Johnson ATC (2011) A carbon nanotube immunosensor for *Salmonella*. AIP Adv 1(4):042127. https://doi.org/10.1063/1.3658573
12. Zhao Z, Lei W, Zhang X, Wang B, Jiang H (2010) ZnO-based amperometric enzyme biosensors. Sensors 10:1216–1231. https://doi.org/10.3390/s100201216
13. Malik P, Katyal V, Malik V, Asatkar A, Inwati G, Mukherjee TK (2013) Nanobiosensors: concepts and variations. ISRN Nanomater. https://doi.org/10.1155/2013/327435
14. Ansari SA, Husain Q (2011) Bioaffinity based immobilization of almond (*Amygdalus communis*) β-galactosidase on con A-layered calcium alginate-cellulose beads: its application in lactose hydrolysis in batch and continuous mode. Iran J Biotechnol 9:290–301
15. Paul B, Panigrahi AK, Singh V, Singh SG (2017) A multi-walled carbon nanotube-zinc oxide nanofiber based flexible chemiresistive biosensor for malaria biomarker detection. Analyst 142:2128–2135
16. Lin SY, Chang SJ, Hsueh TJ (2014) ZnO nanowires modified with Au nanoparticles for nonenzymatic amperometric sensing of glucose. Appl Phys Lett 104:193704. https://doi.org/10.1063/1.4875028
17. Samadi M, Shivaee HA, Zanetti M, Pourjavadi A, Moshfegh A (2012) Visible light photocatalytic activity of novel MWCNT-doped ZnO electrospun nanofibers. J Mol Catal A Chem 359:42–48. https://doi.org/10.1016/j.molcata.2012.03.019
18. Meraat R, Ziabari AA, Issazadeh K, Shadan N, Jalali KM (2016) Synthesis and characterization of the antibacterial activity of zinc oxide nanoparticles against *Salmonella typhi*. Acta Metall Sin (English Lett) 29:601–608. https://doi.org/10.1007/s40195-016-0439-5
19. Cullity BD (1978) Elements of X-ray diffraction, 2nd edn. Addison-Wesley, Phillippines
20. Juan JC, Jiang Y, Meng X, Cao W, Yarmo MA, Zhang J (2007) Supported zirconium sulfate on carbon nanotubes as water-tolerant solid acid catalyst. Mater Res Bull 42:1278–1285. https://doi.org/10.1016/j.materresbull.2006.10.017
21. Zhang X, Fu J, Zhang Y, Lei L (2008) A nitrogen functionalized carbon nanotube cathode for highly efficient electrocatalytic generation of $H_2O_2$ in Electro-Fenton system. Sep Purif Technol 64:116–123. https://doi.org/10.1016/j.seppur.2008.07.020
22. Alias SS, Ismail AB, Mohamad AA (2010) Effect of pH on ZnO nanoparticle properties synthesized by sol-gel centrifugation. J Alloys Compd 499:231–237. https://doi.org/10.1016/j.jallcom.2010.03.174
23. Garg P, Singh BP, Kumar G, Gupta T, Pandey I, Seth RK, Tandon RP, Mathur RB (2011) Effect of dispersion conditions on the mechanical properties of multi-walled carbon nanotubes based epoxy resin composites. J Polym Res 18:1397–1407. https://doi.org/10.1007/s10965-010-9544-8
24. Hu CY, Xu YJ, Duo SW, Zhang RF, Li MS (2009) Non-covalent functionalization of carbon nanotubes with surfactants and polymers. J Chin Chem Soc 56:234–239. https://doi.org/10.1002/jccs.200900033
25. Kavinkumar T, Manivannan S (2016) Synthesis, characterization and gas sensing properties of graphene oxide-multiwalled carbon nanotube composite. J Mater Sci Technol 32:626–632. https://doi.org/10.1016/j.jmst.2016.03.017

26. Mlichová Z, Rosenberg M (2006) Current trends of beta-galactosidase application in food technology. J Food Nutr Res 45:47–54
27. Luo Z, Zhu M, Guo M, Lian Z, Tong W, Wang J, Zhang B, Wei W (2017) Ultrasonic-assisted dispersion of ZnO nanoparticles and its inhibition activity to *Trichoderma viride*. J Nanosci Nanotechnol 18:2352–2360. https://doi.org/10.1166/jnn.2018.14397
28. Ong CB, Annuar MSM (2018) Immobilization of cross-linked tannase enzyme on multiwalled carbon nanotubes and its catalytic behavior. Prep Biochem Biotechnol 48:181–187. https://doi.org/10.1080/10826068.2018.1425707
29. Wibowo KM, Ahmad SA, Sari Y, Saim H, Nurliyana MR, Mansor Z, Sahdan MZ, Muslihati A (2018) The detection method of *Escherichia coli* in water resources: a review. J Phys Conf Ser 995:012065. https://doi.org/10.1088/1742-6596/995/1/012065
30. Li Z, Ma J, Ruan J, Zhuang X (2019) Using positively charged magnetic nanoparticles to capture bacteria at ultralow concentration. Nanoscale Res Lett 14:195. https://doi.org/10.1186/s11671-019-3005-z
31. Hwang JY, Eltohamy M, Kim HW, Shin US (2012) Self-assembly of positively charged carbon nanotubes with oppositely charged metallic surface. Appl Surf Sci 258:6455–6459. https://doi.org/10.1016/j.apsusc.2012.03.060
32. Andrade CAS, Nascimento JM, Oliveira IS, De Oliveira CVJ, De Melo CP, Franco OL, Oliveira MDL (2015) Nanostructured sensor based on carbon nanotubes and clavanin A for bacterial detection. Colloids Surf B Biointerfaces 135:833–839. https://doi.org/10.1016/j.colsurfb.2015.03.037